University of Thi-Qar Journal of Science (UTJsci)
E-ISSN:2709-0256, P-ISSN: 1991-8690, Vol. 13, No. 1, Jun. 2026

Photonic Crystal-Based Biosensor for Measuring Glucose Concentration

Ahmed K. Tebeg*[1,2a] and Hassan A. Yasser[2b]

[1]*Directorate of Education in Thi-Qar, Thi-Qar, Iraq*
[2]*Department of Physics, College of Science, University of Thi-Qar, Nasiriya 64001, Iraq.*

*[a]Corresponding author: ahmed.kareem@utq.edu.iq
[b]Email: hassan.yasser@sci.utq.edu.iq

Received: 30-07-2025, Revised:28-08-2025, Accepted: 19-09-2025, Published: 01-06-2026

***Abstract*—This work clearly demonstrated a response to changes in glucose concentration via a linear shift of the resonance wavelength with increasing concentration. The photonic crystal-based sensor was constructed using COMSOL based on the finite element method. Furthermore, it was shown that as the radius of the silver rod increased, plasmonic interferences and increased scattering caused the resonance spectrum (FWHM) to broaden and the quality factor to decrease. It was also shown that changing the radius (r1) of the photonic crystal material had an impact on the maximum transmittance, resonance wavelength, and spectrum width. Research findings showed that the largest detection limit was $2.25 \cdot 10^{-4}$ RIU, and the best sensitivity was 500 nm/RIU at r1 = 0.123 µm. GaAs had the shortest spectrum width and best sensitivity, while TiO2 had the widest spectral range and the highest detection limit. These results suggested that the sensor could be a useful tool for accurately measuring glucose levels.**

***Keywords*— photonic crystal, biosensor, glucose, sensitivity.**

I. INTRODUCTION

Diabetes is a chronic metabolic ailment emanating from the imbalance in sugar levels in the blood due to the insufficient production of insulin and its inability to be utilized effectively by the body [1]. The hormone insulin, which the pancreas secretes, regulates the amount of sugar in the blood, and disruption can lead to hypoglycemia or hyperglycemia. The former entails blood sugar levels below 40 mg/dL, whereas the latter describes an excess of blood sugar beyond the normal severe range between 270-360 mg/dL [2- 3]. Two main types of diabetes exist: type 1 and type 2. Any of them can lead to several health complications. Among these are renal failure, blindness, deafness, foot and leg damage, and amputations [4]. In addition several other complications that endanger human health to a great extent. The estimated number of adults aged 20-79 living with diabetes is approximately 463 million people, representing 9.3% of this age group worldwide [5].Diabetes management involves invasive and costly constant monitoring of blood glucose levels usually by a method that includes pricking fingertips, which therefore translates the costly, inconvenient, and psychologically demanding to the patient [7]. Animating this process is the fact that researchers are racing to develop more modern technologies like AI-based pancreas systems and continuous glucose monitoring devices, which will make better outcomes even more attainable and decrease risks even further [8-9]. Therefore, other strategies include the development of non-invasive electrochemical and optical biosensors [10- 11]. In this context, biosensors, including photonic crystal-based biosensors, provide sensitive, low-cost, and real-time glucose monitoring, thus potentially transforming diabetes management [12]. Another research direction has explored the application of near-infrared spectroscopy, whereby blood glucose levels can be monitored through the skin via non-surgical methodologies [13- 14]. This technique uses light sources of particular wavelengths and photodiode receivers to detect the reflected light, which is processed by microcontrollers to determine glucose concentration [15].Due to their unique optical properties of periodic structures, the photonic crystal-based biosensor is also an application of these biosensors that is capable of detecting subtle changes in glucose concentration [16-17]. These biosensors are remarkably efficient and responsive, and they can be utilized for real-time detection and data collection [18]. Such development of technology is required to enhance the quality of life of diabetic patients. Appropriate and timely diabetes care can prevent the most serious complications and mortality from diabetes. Although there is a disease, there are research and innovations in biosensors, devices for continuous glucose monitoring [19- 20] and non-invasive tests [21- 22]. which can help to create even more effective and more convenient user solutions for treated patients.

II. SENSOR DESIGN

The sensor is designed by arranging rods, with radius (r1), of one of the materials (GaAs, InP, or TiO2) separated by a distance (a), through the surrounding medium (air).

https://doi.org/10.32792/utq/utjsci/v13i1.1460

The rod arrangement required to make the photonic crystal property is 17 rows and 23 columns [23]. Then a row of these rods was deleted to generate a bus guide located in its first half in the seventh row and its second half in the eleventh row. A group of column elements was also deleted to connect the two busguides. Then a square with a side length of (d) is placed in the middle of the bus guide. The task of this square is to contain the liquid to be tested (which is blood). To increase the efficiency of the sensor by achieving the plasmonic property, two silver rods were added with a radius (r) above and below the square and at a distance (z) from the center of the square. It is used silver because [17].it is the best noble element used in this field for the required purpose. Two waveguides separated by a liquid square and two silver rods. At the beginning of the first guide, the field input is port 1, and at the end of the second guide, the field output is port 2. Table I contains all the geometric parameters of the proposed sensor. Note that, changing the sensor parameters during the simulation will be noted in its place. The sensor will be surrounded by a perfectly matched layer (PML). The PML will absorb incident waves without producing reflections at the limits of the computational domain. Even though the computing domain is finite, the PML is made to reduce reflections and accurately imitate an infinite domain. As a rule of thumb, a PML thickness comparable to half the largest wavelength in the simulation usually works well [3].Fig. 1 illustrates the schematic architecture of the glucose sensor, while Fig. 2 depicts the schematic representation of the sensing system, which comprises various components including an optical source, a photonic crystal-based biosensor, a light detector, a signal processing unit, and a display.

TABLE 1. Simulation parameters of the present structure

parameter	Value	Parameter	Value
L_1	*16μm*	a	*0.667μm*
L_2	*12μm*	r_1	*125nm*
r	*90nm*	λ	*1520nm*
D	*1.59 μm*	z	*1.35 μm*
C	*80mg/ dl*		

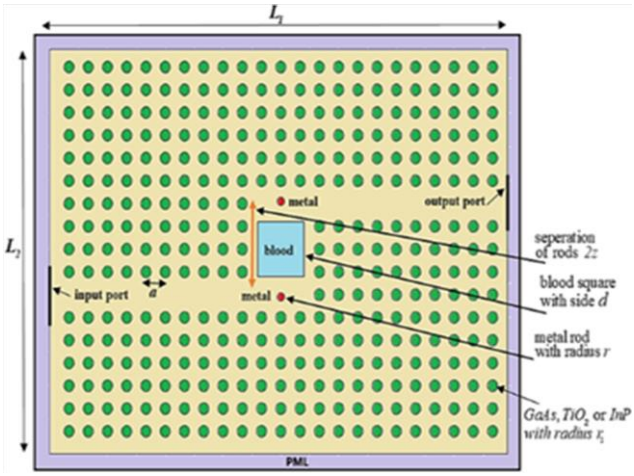

Fig. 1: Present photonic crystal biosensor structure.

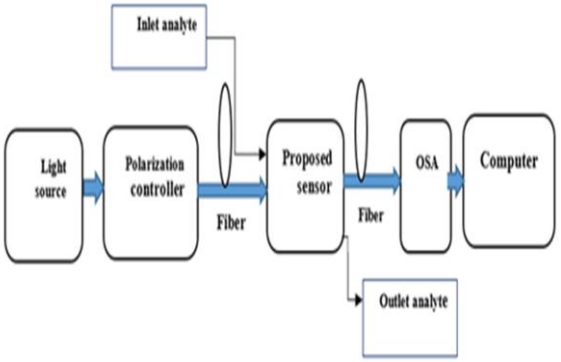

Fig.2: Schematic representation of the usual sensing system configuration

II. SENSOR MATERIALS AND METERS

The sensor is usually made of a combination of materials depending on its intended use, and in this section, we will discuss the properties of materials that can be used in building photonic crystal sensors. The refractive index (n) of blood varies with wavelength over diabetes and other factors and falls in the range of 1.34 to 1.38, with an average value of 1.35[23]. The concentration of glucose in units of mg/dL or mmol/L is a very important measurement in medicine and biochemistry. Normal fasting blood glucose values are between 70 and 100mg/dL (3.9 and 5.6mmol/L)[20]. Ways in which the level of glucose is affected include diet, exercise, hormones, and diseases. There are two ways by which the measurements are to be made, one involving blood index of blood changes with changes in the wavelength of light (λ), glucose concentration (*C*), and temperature (*T*) [1, 2]. At a constant temperature T=37^{o} and a glucose concentration of 80mg/dL, the refractive index is directly proportional to the wavelength, according to the relation [14].

$$n(\lambda)=\sqrt{1+\frac{0.83432\lambda^2}{\lambda^2-10775.44775}+\frac{0.04296\lambda^2}{\lambda^2-6.13587\times10^6}} \quad (1)$$

Where λ is the wavelength in nm. The refractive index of blood as a function of temperature, wavelength and glucose concentration C is given by the relationship [23].

$$n(C,\lambda,T)=n(\lambda)+\alpha\,(C-80)-\beta(T-37) \quad (2)$$

where $\alpha=1.541\times10^{-4}dL/mg$. The third term is to account for the effect of temperature, where

$$\beta=1.051\times10^{-4}(1/C^{o}) \quad (3)$$

In general, we will assume that the temperature is constant at T=37^{o} and that the variables are the wavelength and the glucose concentration.

Gallium arsenide (GaAs) is a semiconductor with a direct band gap, which makes it an ideal material for a variety of applications, including light and laser sources. TheGaAs[27]. Allows for efficient emission of light and has high electron mobility, which makes it perfect for use in biosensing applications. Moreover, theGaAs is highly resistant to oxidation [28]. This type of semiconductor is particularly interesting for the production of light sensors due to their capability of forming nanostructures like quantum dots, as well as their ability to effectively absorb near-infrared radiation[28].The GaAs may have a higher production cost than silicon, but it is still considered a great value for optical, photonic technology, and medical diagnostics. It's true that GaAs's cost, as well as its brittleness, is higher than that of other materials, but it remains a popular choice for high-speed, high-frequency, and optoelectronic applications. The refractive index of GaAs can be defined as [16- 17].

$$n_{GaAs} = \sqrt{5.3725 + \frac{5.4667\lambda^2}{\lambda^2 - 0.1964} + \frac{0.0243\lambda^2}{\lambda^2 - 0.7649} + \frac{1.9575\lambda^2}{\lambda^2 - 13628}} \quad (4)$$

Indium Phosphate (InP) has a direct band gap allowing it to work as a high-electron mobility semiconductor. This property makes it one of the most sought-after materials in the singular interfaces with the III-V system [14]. The (InP) is widely used in substrate metallization of other III-V semiconductors. Indium Phosphate has found major applications in the making of high-speed transistors, optical circuits, LEDs, and components of laser diodes used in fiber optics communication systems. InP is also important for the sensors used in medicine and environmental monitoring where optical sensors are helpful. In the wavelength range from to, the (n) can be calculated as [24].

$$n_{InP} = \sqrt{7.255 + \frac{2.316\lambda^2}{\lambda^2 - 0.6263^2} + \frac{2.765\lambda^2}{\lambda^2 - 32.935^2}} \quad (5)$$

Titanium dioxide (TiO_2) is a white powder known for its advantageous photo-catalytic features, chemically inert and is used in cosmetics, paints, plastics, and others. It does not pose health dangers, and its economic cost is appealing. It neither undergoes modification in acidic nor basic environments. Rutile, brookite, and sphalerite are types of crystalline forms of titanium dioxide, rutile contains the highest refractive index and birefringence. It is for optical utilization with visible and infrared rays. Its potency as a white colourant in addition to polarized optics is due to its high absorption coefficient and light scattering properties coupled with being effectiveness [25].

The optical silver properties are more intense in research since they show selective absorption in the visible and near-infrared ranges. Among the different metals, silver gives the highest efficiency for localized surface plasmon resonance (LSPR) excitation over a very broad wavelength range and much sharper plasmon resonance bands compared to gold. Dissipative loss is also much lower in silver because of its relatively high refractive index compared to gold. These properties can further be tuned by playing the size, shape, and surrounding dielectric environment of nanostructures. Silver is very important in biological sensing due to its antibacterial activity. It is, thus, very important in the sensitive detection of surface plasmon resonance; this makes silver very important in the development of optical and biochemical sensors. Despite the recent difficulties, progress in the methods of surface treatments and silver nanoparticles carries on, promising it a place in the future sensors of high performance [26].

There are many metrics used to judge the quality of a sensor, and using a single metric relation may not give an adequate description of its properties. The spectral sensitivity is defined as the wavelength shift per unit of the refractive index [3].

$$S = \frac{\Delta\lambda_{peak}}{\Delta n_a}\left(\frac{nm}{RIU}\right) \quad (6)$$

Where $\Delta\lambda_{peak}$ refers to the wavelength difference in resonance peaks and Δn_a indicates the change in two adjacent refractive indexes of an analyte (glucose concentrations).

The quality factor is the ratio of the resonant wavelength (λ_{res}) to the full width at half maximum (FWHM) of the achieved transmission spectra [26].

$$Q = \frac{\lambda_{res}}{FWHM} \quad (7)$$

Another important characteristic of optical biosensors is the detection limit (DL), which is the minimum measurable change in

$$DL = \frac{FWHM}{10S} \quad (8)$$

Factor 10 is empirical and may vary depending on the specific application or instrument. It is an essential performance metric, particularly in applications like chemical detection, environmental monitoring, and biosensing. The DL of a homogeneous sensor can be defined as the smallest change in the RI that the sensor can detect. Depending on the design and quality factor, photonic crystal sensors can reach a detection limit of 10^{-4} -$10^{-}10^{-6}$ RIU[30]. The detection limit of a sensor entirely depends on the actual performance of sensitivity and quality factor indicators. The higher the sensitivity and the larger the quality factor, the lower the minimum amount or concentration of a component that can be detected [23].

IV. RESULTS AND DISCUSSION

The photonic crystal sensor is designed using a COMSOL environment based on finite element method (FEM), where a fine mesh size is used to obtain more accurate results. A large number of simulations have been performed with many changes in the geometrical parameters and we highlight the cases that achieve clear changes in the results. The material GaAs was adopted as the basis for building the photonic crystal in all simulations except where mentioned in the appropriate place regarding the use of other materials. Fig. 3 Shows the electric field distribution through the sensor using two

wavelengths λ=1.51µm and λ=1.52µm. It is clear from the distribution that the electric field cannot penetrate from the far side of the structure for some wavelengths, as λ=1.51µm, while using wavelength λ=1.52µm will enable the electric field to penetrate. The amount of field penetration and its specificity certainly depend on the rest of the structure parameters.

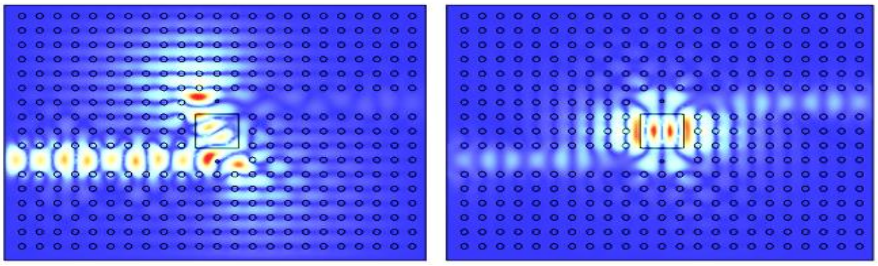

Fig. 3: The corresponding electric field distributions at λ=1.51µm and 1.52µm.

Fig. 4 shows the relationship between the RI of blood and the wavelength for glucose concentrations. Fig. 4(a) represents the relationship between blood absorption rate (RI) and wavelength for three glucose concentrations (80, 120, and 160mg/dL). It is observed that the blood absorption rate decreases with increasing wavelength, and that higher glucose concentrations lead to an increase in the refractive index. This relationship is attributed to the optical and absorption effects of blood components. Regarding the effect of glucose concentration: At certain wavelengths, increasing the glucose concentration in the sample leads to an increase in the blood absorption rate. Fig. 4(b) shows the relationship between the refractive index of blood and glucose concentration at different wavelengths (0.5, 1, 1.5, and 2 µm) in mg/dL. All curves show a linear increase in the refractive index with increasing concentration. This indicates that the concentration of substances in the blood directly affects the optical properties. Therefore, it can be concluded that the refractive index increases with increasing concentration, which may be useful in optical systems for accurately determining concentration properties. The longer the wavelength, the lower the refractive index, indicating the effect of light scattering within the blood at shorter wavelengths. Fig. 5 shows the relationship of transmittance to wavelength for three glucose concentrations using two values of the silver rod radius *r*. Fig. 5(a) shows that increasing the glucose concentration will shift the curve to the right while keeping the value of the peak of the curve almost constant. The RI of the medium is affected by increasing the concentration of glucose, and the resonance wavelength is shifted towards longer wavelengths. Physically, the energy required for resonance reduces by increasing the RI, causing the peak to shift to higher wavelengths. As the radius of the silver rod increases, Fig. 5(b), the behavior repeats itself with peaks occurring at different wavelengths and increasing FWHM. The properties of the surface plasmons are affected by increasing the radius of the silver rod resulting in an increased spectral bandwidth, whereas the larger rod allows for greater overlap between the surface plasmon modes, resulting in a broader absorption range and spectral response.

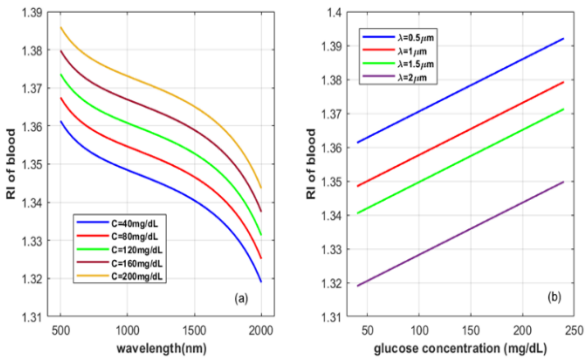

Fig. 4: a) RI of blood as a function of wavelength for many glucose concentration, b) RI of blood as a function of glucose concentration for many wavelengths

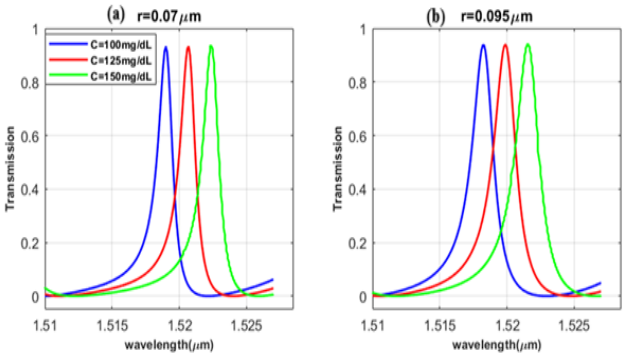

Fig. (5): The transmission as a function of wavelength for three glucose concentrations using two values of r: a) r=0.07µm and b) r=0.095µm.

Fig. 6 shows the FWHM, resonant wavelength, quality factor and resonant transmittance as functions of sugar concentration for three values of silver rod radius. Fig. 6(a) shows that the spectral width increases with increasing glucose concentration and that increasing the silver rod radius causes a clear increase in the achieved spectral width. Physically, increasing the radius of the silver rod results in an increase in the FWHM due to the effect of radiation damping and increased scattering losses. As the radius increases, the plasmonic interactions increase, leading to a broadening of the absorption band and a decrease in resonance selectivity. The effect of glucose concentration increases the RI, causing additional changes in the plasmonic response and leading to an increase in the bandwidth with increasing concentration. Fig. 6(b) shows that the resonant frequency increases linearly with increasing glucose concentration and that increasing the

radius of the silver rod slightly reduces the achieved resonant frequencies. A linear relationship is a desirable property in the field of sensors. Increasing the glucose concentration leads to a higher RI, which causes a linear shift towards longer wavelengths in the resonant wavelength. The effect of increasing the radius of the silver rod leads to a modification of the local surface plasmon response (LSPRs), where the resonant wavelength increases but at a lower rate compared to the effect of glucose. This is because the larger size reduces the sensitivity of the particles to changes in the RI of the surrounding environment, which makes the lines closer together but still follow the same general trend. Fig. (6c) shows the quality factor which decreases slightly with increasing glucose concentration for different silver rod radii. In general, we see that increasing the silver rod radius causes a clear decrease in the quality factor of the system and this is attributed to the increase in interactions with the field and scattering. Fig. (6d) represents the resonance transmittance achieved with each glucose concentration, and it appears to increase slightly with increasing concentration or remain constant for larger silver rod radii. We notice that the transmittance here is greater for larger radii but at the expense of the achieved spectral width and quality factor. In general, a trade-off can be made to obtain satisfactory results for the application being used.

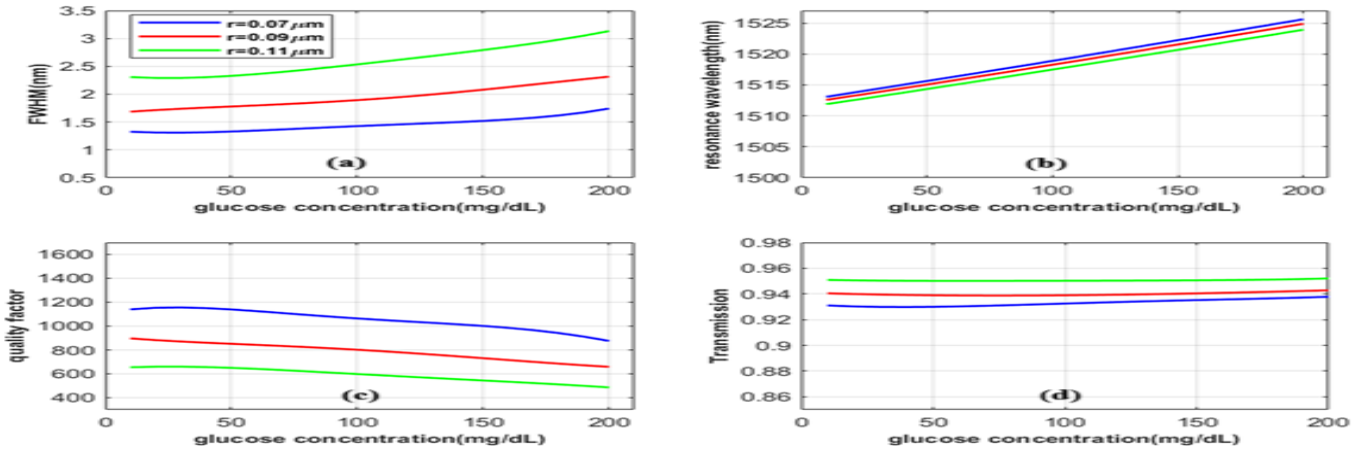

Fig. 6:FWHM resonance wavelength, quality factor and transmission as functions of glucose concentration using many *r* values.

Fig. 7 represents the relationship of spectral width, resonant wavelength and maximum transmittance as a function of r_1 for three glucose concentrations, where r_1 represents the radius of the material from which the photonic crystal is composed. In Fig. 7(a), the spectral width starts at a certain value, decreases slightly and then starts to increase with the radius r_1, on the other hand, increasing the glucose concentration causes an increase in the overall spectral width values in the same manner mentioned previously. In Fig. 7(b), there is a similar behavior for the change in the resonant wavelength with increasing r_1. Increasing the glucose concentration will also cause a general increase in the resonant wavelength. Fig. 7(c) represents the maximum transmittance achieved as a function of r_1, and there is a slightly wavy relationship with a slight increase with increasing r_1. The maximum transmittance achieved is at the highest glucose concentration. In general, changing (r_1) causes clear changes and this is attributed to the change in the properties of the photonic crystal.

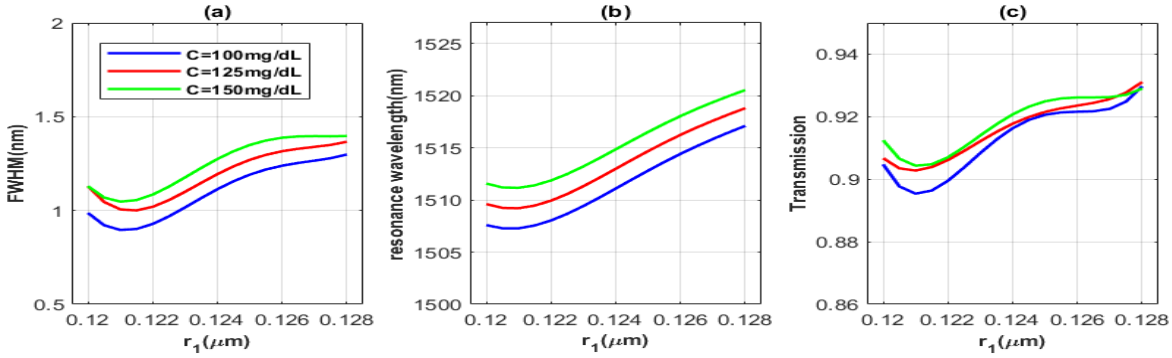

Fig.7: FWHM, resonance wavelength and peak transmission as functions of r_1 using different glucose concentrations.

Fig. 8 shows a plot bar of the sensitivity achieved for three values of *z*, where *z* refers to the distance from the blood square's center to the silver rod's center. We see in all cases that the sensitivity achieved is within the range of 400-450mg/dL, with slight changes as *z* changes. This achieved range of sensitivity is considered good in the field of sensors. The closeness of the values achieved means that the sensor works for all glucose concentrations in almost the same way. Fig. 9 represents the corresponding detection limits plot bar for Fig. 8, and it is seen that the detection limits are in the range 2.75×10^{-4} - 4.25×10^{-4} RIU. The subfigures are almost identical, but case z=1.42μm gives the best convergence values. These resulting limits are very acceptable in the field of photonic

crystal sensors. Fig. 10 shows plot bars of the best sensitivity and detection limit achieved for the case r_1=0.123µm, where r_1 represents the radius of the rods of the material composing the photonic crystal. The achieved sensitivity rate of 500mg/dL and the corresponding detection limits are about 2.25×10^{-4} RIU. Fig. 11 represents the plot bars of the sensitivity and detection limit achieved for the case d=1.6µm, where d represents the radius blood square in the structure. In this case, the achieved sensitivity rate of 425mg/dL and the corresponding detection limits are about 3.5×10^{-4} RIU. Fig. 12 obtains the plot bars of the best sensitivity and detection limit reconstructed at the case r=0.07µm, where r represents the radius of metal rods. In this case, the verified sensitivity rate of 425mg/dL and the corresponding detection limits are about 3.1×10^{-4} RIU

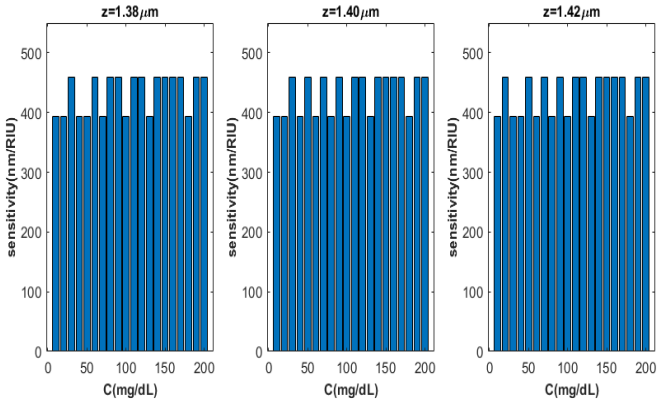

Fig. 8: Sensitivity plot bar at different glucose concentrations using different using many z values.

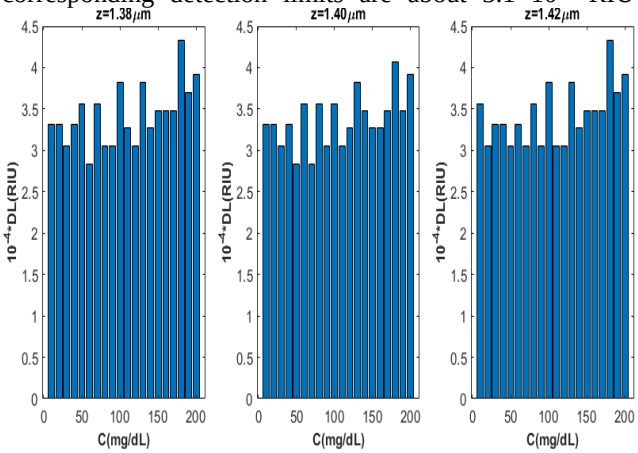

Fig.9 :Detection limit plot bar at different glucose concentrations using many z values.

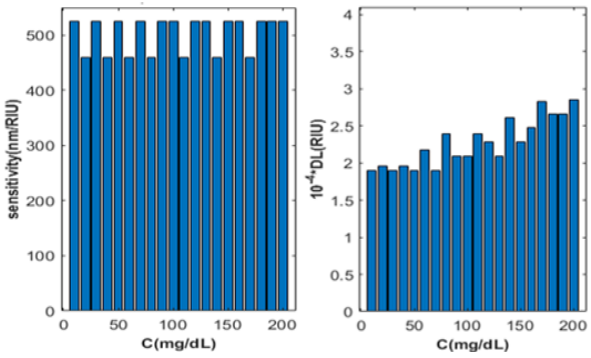

(a) (b)

Fig. 10 :The plot bars at different glucose concentrations of:
a) sensitivity and b) detection limit using d=1.6µm.

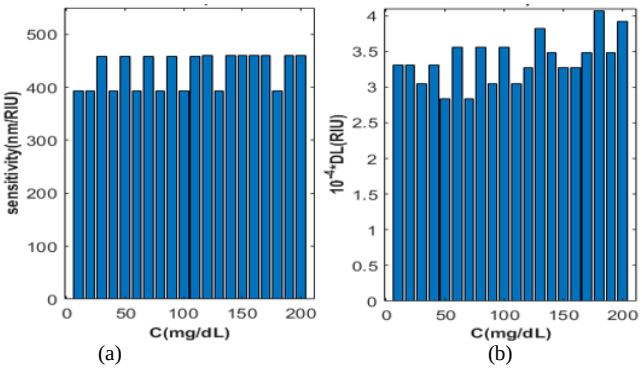

(a) (b)

Fig. 11: The plot bars at different glucose concentrations of:
a) sensitivity and b) detection limit using r_1=0.123µm

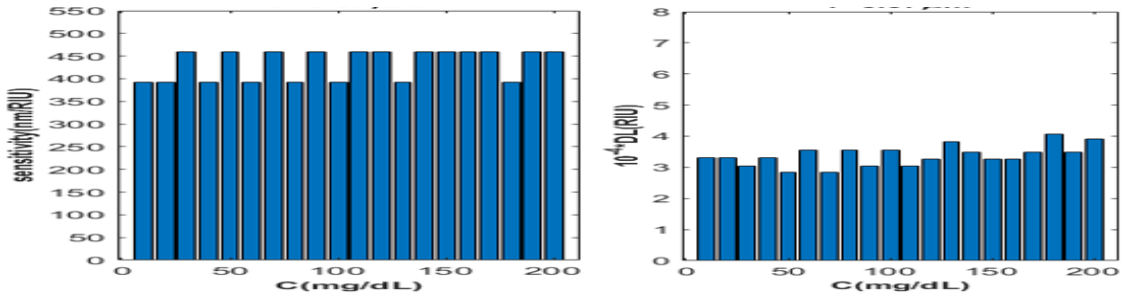

(a) (b)

Fig. 12: the plot bars at different glucose concentrations of: a) sensitivity and b) detection limit using r=0.07µm.

Fig.13 shows the FWHM, resonant wavelength, quality factor and resonant transmittance as functions of sugar concentration using the following three materials as the basis for the photonic crystal: InP, GaAs, and TiO_2. Fig. 13a shows that the spectral width changes significantly depending on the material forming the photonic crystal, where GaAs show a very small spectral width followed by InP and TiO_2 with the highest spectral width. This is attributed to the difference in the material properties and refractive index at the wavelength used. Fig. 13(b) shows that the relationship of resonant wavelength with glucose concentration is still linear, where the material with the highest resonant wavelength has the smallest spectral width and vice versa. Fig. 13(c) shows that the variation of

quality factor with glucose concentration is still linear, where the material with the highest resonant wavelength has the smallest spectral width and vice versa. The decreasing quality factor approximately has a certain fluctuation as the glucose concentration increases. We notice that the quality factor values achieved for the different materials come in reverse order compared to the spectral width. Fig. 13(d) shows that the maximum transmittance increases with increasing glucose concentration. We notice that the values of the maximum transmittance achieved for the different materials come in reverse order compared to the resonance wavelength.

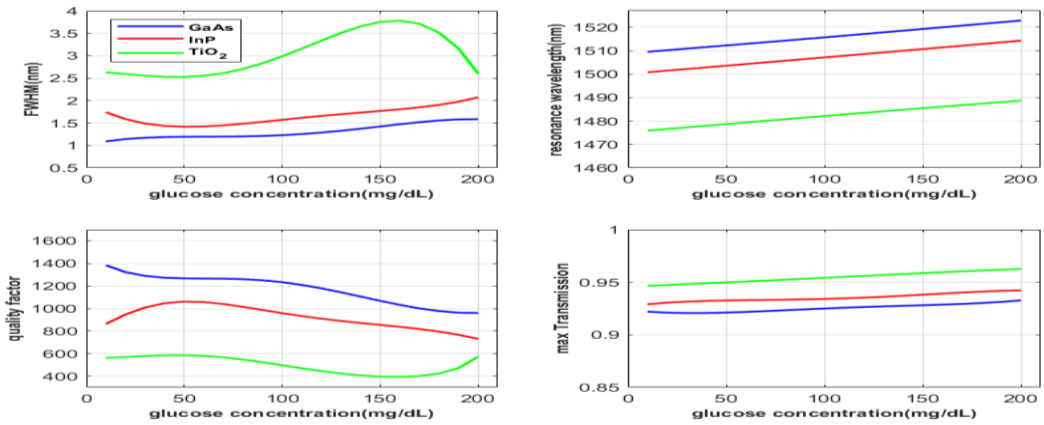

Fig. 13: FWHM, resonance wavelength, quality factor and transmission as functions of glucose Concentration using many materials, where d=1.6µm, z=1.4µm, r=0.07µm and r_1=0.129µm.

Figs. (14) and (15) represent the sensitivities and the corresponding detection limits, respectively, for different materials. Fig. (14) shows that the sensitivity has an average of approximately 450nm/RIU for all materials with individual values appearing to have slightly different values. On the other hand, Fig. 15 shows that the detection limit is very low at about 2.1×10^{-4} RIU for InP material, and slightly higher for GaAs material, while TiO_2 material has a very high detection limit at about 7×10^{-4} RIU. Also, the resulting values for the detection limits are close to each other for materials Inp and GaAs but very different for TiO_2 material.

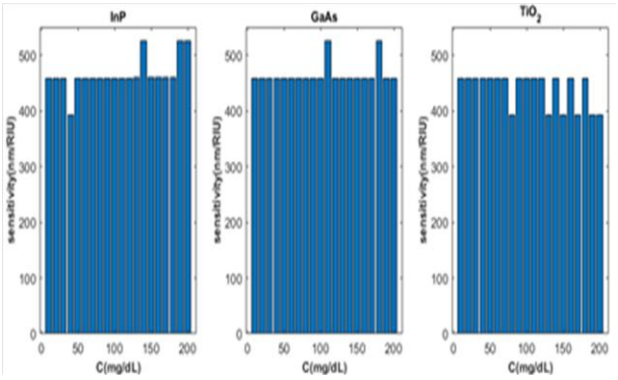

Fig. 14: Sensitivity plot bar at different glucose concentrations using different using many materials, where d=1.6µm, z=1.4µm, r=0.07µm and r_1=0.129µm.

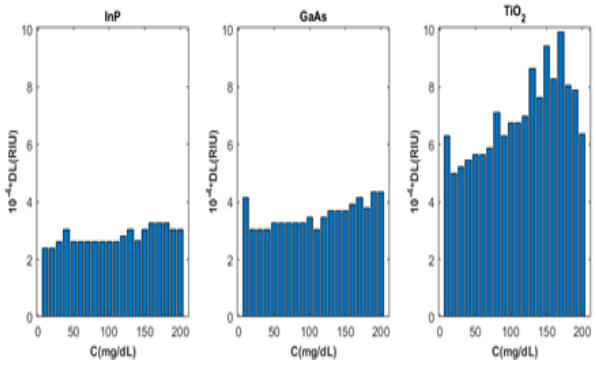

Fig. 15: Detection limit plot bar at different glucose concentrations using different using many materials, where d=1.6µm, z=1.4µm, r=0.07µm and r_1=0.129µm

Many scientific efforts are working on using photonic crystals as sensors for various applications. Table II compares the proposed biosensor and other sensors. Compared with the aforementioned sensors, the proposed structure achieved a relative balance between the sensitivity and the quality factor

TABLE 2. Comparison of the Proposed Structure with other Biosensor.

Reference	Quality factor	Sensitivity (nm/RIU)	Maximum transmission %	FWHM (nm)	DL (RIU)
R. Arunkumar et al. [28]	262	N/A	97	6	20×10^{-4}
A. Asuvaran and G. Elathrasan [29]	573	4615	95	N/A	13×10^{-4}
R. Kumar et al. [30]	650	850	N/A	N/A	N/A
Y.Yang etal. [27]	980	915	99	N/A	2.36×10^{-4}
This work	1400	500	97	1	2.25×10^{-4}

VI. CONCLUSIONS

In conclusion, the sensor performance depends on: wavelength, glucose concentration, and geometrical dimensions. The resonant wavelength has a linear relation with glucose concentration, which facilitates accurate measurement. Increasing the radius of the silver rod increases the width of the resonant spectrum and reduces the quality factor due to scattering effects and plasmonic interferences. The choice of the material of the photonic crystal greatly affects the performance, with GaAs providing accurate response and high sensitivity, while TiO_2 has a wider spectral range and a higher detection limit. A sensitivity of 500 nm/RIU and a very low detection limit of 2.25×10^{-4} RIU were achieved, making the sensor suitable for medical applications. The stable performance when the z-distance between the center of the sample and the silver rod changes indicates the possibility of using the sensor in reliable measurements of various glucose concentrations. The results demonstrate the possibility of adjusting the geometric and material parameters of the sensor to obtain the best possible sensitivity and accuracy. The designed sensor is efficient and scalable to be part of high-precision medical sensing systems for detecting glucose concentrations.

ACKNOWLEDGMENT

We would like to thank the organizations and individuals for their participation in this study, including the Gastrointestinal tract Teaching Hospital/Medical city, Baghdad and Azadi Teaching Hospital/Hepatitis unit, Kirkuk, in addition to Kidney dialysis center in Kirkuk Teaching Hospital, as well as all the volunteers who generously donated their time to help with the research. We sincerely appreciate your commitment and contribution.

CONFLICT OF INTEREST

The authors declare that they have no conflict of interest.

REFERENCES

[1] H. Wang, J. Yi, Y. Yu, and S. Zhou, "NIR upconversion fluorescence glucose sensing and glucose-responsive insulin release of carbon dot-immobilized hybrid microgels at physiological pH," *Nanoscale*, Vol. 9, No. 2, pp. 509–516, 2017.

[2] B. Arneth, R. Arneth, and M. Shams, "Metabolomics of type 1 and type 2 diabetes," *International Journal of Molecular Sciences*, Vol. 20, No. 12 pp. 2467, 2019.

[3] H. Yasser and M. Benhaliliba, "A plasmonic photonic crystal fiber sensor with simplified features for identifying unidentified analytes," *University of Thi-Qar Journal of Science*, Vol. 1,No.1, pp. 709–756, 2024.

[4] C. Rubio-Mercedes, N. Cunha, and J. Silva, "Numerical analysis of plasmonic couplers based on metallic lens," *Journal of Microwaves, Optoelectronics and Electromagnetic Applications*, Vol. 22, No. 3, pp. 346–359, 2023.

[5] J. Moses, S. Adibi, N. Wickramasinghe, L. Nguyen, M. Angelova, and S. Islam, "Non-invasive blood glucose monitoring technology in diabetes management: A review," *mHealth*, Vol. 10, No. 9, pp. 9, 2024.

[6] M. Sun, I. Li, W. Lin, and G. Lin, "Pros and cons of continuous glucose monitoring in the intensive care unit," *World Journal of Clinical Cases*, Vol. 9, No. 24, pp. 8666–8670, 2021.

[7] Y. Zhang, S. Chen, Y. Yu, and J. Wang, "A miniaturized photoacoustic device with laptop readout for point-of-care testing of blood glucose," *Talanta*, Vol. 209, No. 1, pp. 120527, 2020.

[8] T. Lin and A. Gal, "Non-invasive glucose monitoring: A review of challenges and recent advances," *Current Trends in Biomedical Engineering and Biosciences*, Vol. 6, No. 3, pp. 1–8, 2017.

[9] Q. Zhao, J. Liu, H. Yang, H. Liu, G. Zeng, B. Huang, and J. Jia, "Double U-groove temperature and refractive index photonic crystal fiber sensor based on surface plasmon resonance," *Applied Optics*, Vol. 61, No. 25, pp. 7225–7230, 2022.

[10] M. Bahadoran, A. Seyfari, P. Sanati, and L. Chua, "Label-free identification of the different status of anemia disease using optimized double-slot cascaded microring resonator," *Scientific Reports*, Vol. 12, No. 1, pp. 1–10, 2022.

[11] B. Liu, Y. Peng, Z. Jin, X. Wu, H. Gu, D. Wei, Y. Zhu, and S. Zhuang, "Terahertz ultrasensitive biosensor based on wide-area and intense light-matter interaction supported by QBIC," *Chemical Engineering Journal*, Vol. 462, no. 1, pp. 142347, 2023.

[12] M. Therese, P. Dharanyadevi, A. Devi, and C. Kalaiarasy, "Detection of blood glucose level in humans using non-invasive method-RL BGM," *International Journal of Recent Technology and Engineering*, Vol. 9, No. 1, pp. 304–309, 2020.

[13] H. Salman and H. Yasser, "Guided Modes in Slab Waveguide with Central Anisotropic Metamaterial Layer," *IOP Conf. Series: Materials Science and Engineering*, Vol. 928, No. 7, p. 072127, 2020.

[14] H. Hameed and H. Yasser, "Three-Layer Slab Waveguide with Chiral Metamaterial Core and Graphene Interfaces," *University of Thi-Qar Journal of Science*, Vol. 11, No. 2, pp. 234–235, 2024.

[15] R. Hani, B. Mahdi, and A. Mohammed, "Photonic crystal fiber sensor for blood with different concentrations of zinc," *Materials Science Forum*, Vol. 1002, No. 2, pp. 290–299, 2020.

[16] Y. Jiang, C. Shi, and J. Wang, “A hybrid plasmonic terahertz waveguide with ridge structure based on bulk-Dirac-semimetal,” *Optics Communications*, Vol. 475, No. 1, pp.233-237, 2020.

[17] F. Wang, Y. Chen, C. Lie, T. Ma, X. Wang, K. Yu, and L. Li, “Ultracompact and broadband mid-infrared polarization beam splitter based on an asymmetric directional coupler consisting of GaAs-CaF2 hybrid plasmonic waveguide and GaAs nanowire,” *Optics Communications*, Vol. 502, No. 1, pp. 203–205, 2022.

[18] J. Lee, M. Kim, and Y. Choi, “Series resistance influence on the performance of waveguide type germanium photodetectors on silicon,” *Chinese Optics Letters*, Vol. 15, No. 15, pp. 100401, 2017.

[19] K. Kolwas and A. Kachova, “Impact of the interband transitions in gold and silver on the dynamics of propagating and localized surface plasmons,” *Nanomaterials*, Vol. 10, No. 12, pp. 1411, 2020.

[20] S. Shaddod and H. Yasser, "Theoretical Study of Sensitivity of Slab-Sensor with Metamaterial," *University of Thi-Qar Journal*, Vol. 14, No. 1, pp. 267–275, 2019.

[21] A. Kadhim and H. Yasser, “Effects of lattice types on the frequency bandwidths in photonic crystals,” *University of Thi-Qar Journal of Science*, Vol. 8, No. 2, pp. 80–85, 2021.

[22] Z. Xing, W. Yang, Z. Yuan, X. Li, Y. Wu, J. Long, S. Jin, Y. Zhao, T. Liu, L. Bian, S. Lu, and M. Luo, “Growth and characterization of high in-content InGaN grown by MBE using metal modulated epitaxy technique (MME),” *Journal of Crystal Growth*, Vol. 516, No. 15, pp. 57–62, 2019.

[23] B. Huard and G. Kirkham, “Mathematical modelling of glucose dynamics,” *Current Opinion in Endocrine and Metabolic Research*, Vol. 25, No. 1, pp. 100379, 2022.

[24] N. Polyanskiy, "Refractiveindex.info database of optical constants," *Scientific Data*, Vol. 11, No. 21, pp. 94, 2024.

[25] A. Uniyal, B. Chauhan, A. Pal, and V. Srivastava, “InP and graphene employed surface plasmon resonance sensor for measurement of sucrose concentration: A numerical approach,” *Optical Engineering*, Vol. 61, No. 5, pp. 057103, 2022.

[26] H. Ali, H. Ammar, and H. Yasser, “Metal type effect on plasmonic fiber properties,” *IOP Materials Science and Engineering*, Vol. 31, No. 2, pp. 76, 2020.

[27] Y. Yang, Y. Xiang, and X. Qi, “Design of photonic crystal biosensors for cancer cell detection,” *Micromachines*, Vol. 14, No.6, pp. 1478, 2023.

[28] R. Arunkumar, T. Suaganya, and S. Robinson, “Design and analysis of 2D photonic crystal-based biosensor to detect different blood components,” *Photonic Sensors*, Vol. 9, No. 1, pp. 69–77, 2019.

[29] A. Asuvaran and G. Elathrasan, “Design of two-dimensional photonic crystal-based biosensor for abnormal tissue analysis,” *Silicon*, Vol. 14, pp. 7203–7210, 2022.

[30] R. Kumar, G. Bharti, and R. Bindal, “Modeling and simulation of an optical sensor for cancer cell detection,” *International Journal of Electrical and Electronics Research*, Vol. 10, No.3,pp. 792–795, 2022